



HAL
open science

Strengthening Peptoid Helicity through Sequence Site-Specific Positioning of Amide Cis-Inducing Nt Bu monomers

Maha Rzeigui, Mounir Traïkia, Laurent Jouffret, Alexandre Kriznik, Jameleddine Khiari, Olivier Roy, Claude Taillefumier

► **To cite this version:**

Maha Rzeigui, Mounir Traïkia, Laurent Jouffret, Alexandre Kriznik, Jameleddine Khiari, et al.. Strengthening Peptoid Helicity through Sequence Site-Specific Positioning of Amide Cis-Inducing Nt Bu monomers. *Journal of Organic Chemistry*, 2020, 85 (4), pp.2190-2201. 10.1021/acs.joc.9b02916 . hal-02430577

HAL Id: hal-02430577

<https://hal.univ-lorraine.fr/hal-02430577>

Submitted on 3 Feb 2022

HAL is a multi-disciplinary open access archive for the deposit and dissemination of scientific research documents, whether they are published or not. The documents may come from teaching and research institutions in France or abroad, or from public or private research centers.

L'archive ouverte pluridisciplinaire **HAL**, est destinée au dépôt et à la diffusion de documents scientifiques de niveau recherche, publiés ou non, émanant des établissements d'enseignement et de recherche français ou étrangers, des laboratoires publics ou privés.

“Strengthening Peptoid Helicity through Sequence Site-Specific Positioning of Amide Cis-Inducing *NtBu* monomers”

Maha Rzeigui,^{a,d} Mounir Traikia,^a Laurent Jouffret,^a Alexandre Kriznik,^{b,c}
Jameleddine Khiari,^d Olivier Roy,^a and Claude Taillefumier^{*,a}

^a*Université Clermont Auvergne, CNRS, SIGMA Clermont, ICCF, F-63000 Clermont-Ferrand, France*

^b*Université de Lorraine, CNRS, IMoPA, F-54000 Nancy, France*

^c*Université de Lorraine, CNRS, Inserm, UMS2008 IBSLor, Biophysics and Structural Biology core facility, F-54000 Nancy, France*

^d*Université de Carthage, Faculté Des Sciences de Bizerte, Laboratoire de Chimie Organique et Analytique, ISEFC, 2000, Bardo, Tunisie*

corresponding author : claudetaillefumier@uca.fr

Keywords: Peptoids; Polyproline type I helix, Cis-trans isomerization; Peptidomimetics

ABSTRACT

The synthesis of biomimetic helical secondary structures is sought after for the construction of innovative nanomaterials and applications in medicinal chemistry such as the development of protein-protein interactions modulators. Peptoids, a sequence-defined family of oligomers, enable a peptidomimetic strategy, especially considering the easily accessible monomer diversity and peptoid helical folding propensity. However, cis-trans isomerization of the backbone tertiary amides may impair the peptoid's adoption of stable secondary structures, notably the all-*cis* polyproline I-like helical conformation. Here we show that cis-inducing *NtBu* achiral monomers strategically positioned within chiral sequences may reinforce the degree of peptoid helicity, although a reduced content of chiral side chains. The design principles presented here will undoubtedly help to achieve more conformationally stable helical peptoids with desired functions.

INTRODUCTION

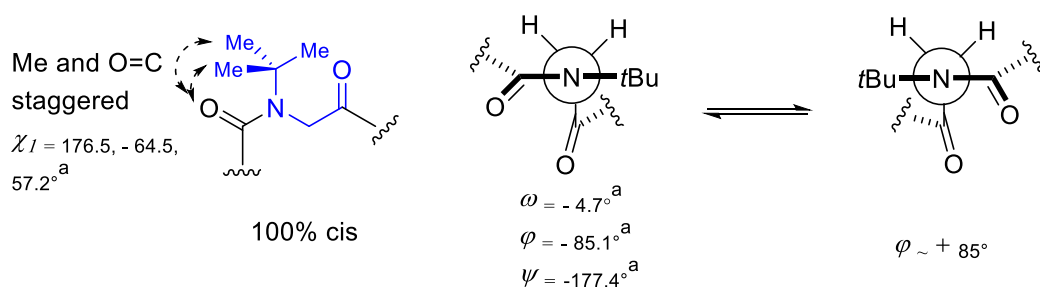
N-substituted glycine oligomers, also called “peptoids” have emerged as a very attractive class of synthetic amide-based oligomers. There are many reasons for this, ranging from their ease of synthesis with unique side chain diversity¹ to their conformational versatility which opens up a wide range of potential applications relevant to biomaterial science^{2,3}, therapeutics development,^{4,5,6} and catalysis.^{7,8,9}

Peptoids should be regarded as biotic foldamers since their backbone closely resembles that of peptides with the side chains attached to the amide nitrogen atoms rather than the C α carbons, and also because single-chain peptoids may exhibit biopolymer-like conformational behaviours. The iterative “submonomer” method¹⁰ used to synthesise peptoids generates sequence-defined oligomers with protease-resistant tertiary amide bonds,^{11,12} a desirable property for developing peptidomimetic ligands and biomimetic discrete secondary structures. Peptoids have been shown to fold in a variety of secondary structures, some of which are reminiscent those of peptides, like helices, sheets and turns,^{13,14,15,16,17,18,19} and others are singular like square helices and ribbons.^{20,21,22} However, *cis-trans* isomerisation of the peptoid tertiary amide bonds (*N,N*-disubstituted amides) is a source of conformational heterogeneity^{23,24} which may impair the formation of well-defined secondary structures. A number of research groups have engineered peptoid side chains that allow a local control of the dihedral angles through a set of backbone to side chain and side chain to side chain weak non-covalent interactions.^{25,26,27,28,29,30,31} Two peptoid helical conformations have been characterized; one of them has an overall shape resembling the naturally-occurring polyproline II, an extended all-*trans* helix most frequently occurring in proline-rich sequences. The other one resembles the all-*cis* polyproline I helix (PPI) which is characterised by a three-fold periodicity and a helical pitch of approximate to 6 Angstrom. The latter has been observed for proline-rich sequences in hydrophobic solvents, like *n*-PrOH.³² Zuckermann was the first to uncover the role of *N* α chiral aromatic peptoid side chains, typically (*S*)- or (*R*)-1-phenylethyl (*spe/rpe*) side chain, on the folding into the PPI-like conformation.³³ (*S*)-*N*-(1-phenylethyl)glycine monomers are, for example, commonly used to induce right-handed helices.^{9,34,35} Sequence requirements and chain length effects were carefully studied which established the rules for the formation and stabilisation of chiral PPI-type helical secondary structures from aromatic-containing monomers.^{36,37,38} In contrast, the control of peptoid helicity from non-aromatic monomers has been much less investigated.^{14,30} Recently we started to explore new avenues for stabilizing PPI-like peptoid helices avoiding aromatic side chains. Two novel aliphatic side chains were added to the peptoid “toolbox”, the bulky *tert*-butyl

and *tert*-butylethyl side chains, the monomers of which have been termed *NtBu* and *Ns1tbe* (*S* configuration) (Figure 1). The very bulky *tert*-butyl group is the only one known to lock peptoid amide bonds in the *cis* conformation.²⁹ X-ray crystal structures of *NtBu* oligomers showed their PPI-like helix folding and calculations revealed that this conformation is stabilized through weak non-covalent interactions, notably London interactions between *tBu* side chains located on the same face of the helix.³⁰ Nonetheless, the lack of *NC* α stereogenic center means that the φ dihedral angles may adopt + and – values (around 85°, Figure 1a) which results in conformational heterogeneity in solution. On the other hand, the chiral aliphatic *tert*-butylethyl side chain is one of the best *cis*-peptoid amide inducer allowing the formation of discrete PPI helices of defined handedness.¹⁶

Interestingly, an increase of helicity was observed by CD spectroscopy for the mixed Ac-*NtBu*-(*Ns1tbe*)₄-*NtBu*-*OtBu* and Ac-(*NtBu*)₂-(*Ns1tbe*)₄-(*NtBu*)₂-*OtBu* oligomers, compared to their parent homo-oligomers composed solely of *Ns1tbe* residues. This observation was correlated to an increase of *cis*-amide bonds population for the *Ns1tbe* monomers, suggesting that the two types of monomers can act synergistically to achieve extremely robust helices of defined handedness. Proof of this is the solid state structure of the octamer Ac-(*NtBu*)₂-(*Ns1tbe*)₄-(*NtBu*)₂-*OtBu*, the longest linear peptoid ever solved which revealed a right-handed helix of great regularity despite only a 50% content of chiral monomers. These fascinating results evoking a Sergeant-and-Soldiers behaviour³⁹ encouraged us to pursue our investigations. Here we address the questions of the amount and site-specific placement of achiral *NtBu* glycine monomers within *Ns1tbe* sequences with respect to peptoid helicity. 2D NMR HSQCAD experiments were used to determine the overall backbone amide $K_{cis/trans}$ in deuterated chloroform and acetonitrile and, CD spectroscopy to evaluate variation of peptoid helicity. Two crystal structures are also reported with backbone dihedral angles corresponding to the PPI helix.

a) Achiral *NtBu* monomer



b) Chiral *Ns1tbe* monomer

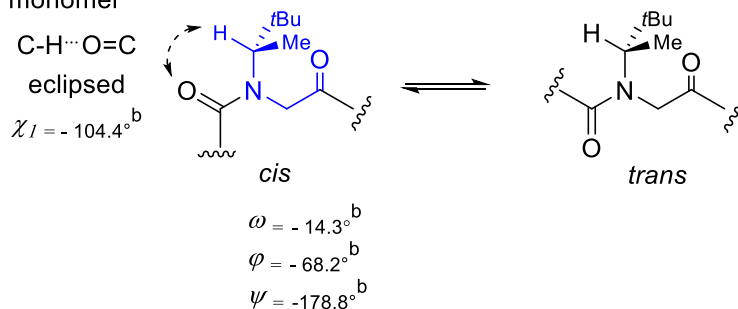


Figure 1. Structure and conformational characteristics of the *NtBu* and *Ns1tbe* peptoid residues used in this study (drawn in blue), see table 2 for the dihedral angles definition. ^aMeasured for the central residue of the crystal structure of H-(*NtBu*)₅-OBn.³⁰ ^bMeasured for the central residue of the crystal structure of Ac-(*Ns1tbe*)₅-OtBu¹⁶. The χ_1 angles have been measured for each *tBu* NC _{β} methyl carbon in case of the representative *NtBu* monomer; the *tBu* NC _{β} has been used for measuring the χ_1 angle (-104.4) in case of the representative *Ns1tbe* monomer.

RESULTS AND DISCUSSION

Design and synthesis of peptoid oligomers 1-16. Recently, we have proposed two efficient structure-inducing peptoid side chains avoiding aromatic groups: the *tert*-butyl (*t*Bu) and (*S*)-1-*tert*-butylethyl (*s*1tbe) side chains. The following two mixed peptoids Ac-*Nt*Bu-(*Ns*1tbe)₄-*Nt*Bu-*Ot*Bu (**A**) and Ac-(*Nt*Bu)₂-(*Ns*1tbe)₄-(*Nt*Bu)₂-*Ot*Bu (**B**) of 6 and 8 residues in length have revealed a remarkable level of helicity.¹⁶ In the initial design, the *Nt*Bu monomers were positioned at the *N*- and *C*-termini of the peptoid chains, and the amount of chiral side chain was 66% for the hexamer and 50% for the octamer. The above results pose several questions: (1) Should the all-*cis* inducing *Nt*Bu monomers be necessarily positioned at the extremities of the oligomers to enhance conformational homogeneity? (2) Is a single *Nt*Bu monomer capable of exerting such control over the conformation, and, if so, at which position should it be placed in the sequence? (3) Considering the initial design with the achiral monomers at the oligomer's end, to what extent the length of the chiral central *Ns*1tbe-based segment can be shortened? Conversely how many consecutive *Nt*Bu residues can be placed at the extremities without affecting chiral induction from the center to both ends of the oligomers. Peptoid helix folding is a chain length-dependent process.³⁷ For example, an increase of ellipticity was observed for *Nr*pe oligomers between 4 and 12 residues in length, suggesting that the helix with *cis*-amide bonds becomes the most favored conformation, only when the oligomer length of 11-13 residues is reached. Designing medium-size peptoids displaying a strong conformational stability is still challenging. For this reason and also because of the remarkable level of helicity of hexamer **A**, we chose to synthesize a first family of peptoid hexamers (**1-6**) enabling us to answer points (1) and (2) (Table 1). Peptoids **7-11** were designed to evaluate how the length of the chiral and achiral segments impact helicity (question 3 above) and peptoids **12-16** were prepared in order to evaluate oligomers composed of the same repeated (*Nt*Bu-*Ns*1tbe-*Ns*1tbe) pattern, thus placing the *t*Bu side chains on the same face of the helical structure. This design is of particular importance since “functional versions” of the *tert*-butyl side chain of structure NC(CH₃)₂CH₂R have been proposed. They allow mimicking amino acid side chains while retaining the conformational properties of the parent *t*Bu group.⁴⁰

In view of the difficulties experienced by our group for the solid-phase synthesis of *Nt*Bu-based oligomers, solution-phase synthesis was preferred in this study.⁴¹ Thus, peptoids **1-16** were synthesized *via* a solution-phase submonomer method (SI, Figure S1). All final compounds were isolated with purity greater than 95%, as determined by integration of peaks with UV detection at 214 nm, after purification by flash silica gel column chromatography or preparative RP-HPLC (see ESI for HPLC data). They were characterized by MS to confirm their identity (Table 1).

Peptoids **1-16** were further analyzed by NMR experiments (^1H , ^{13}C , COSY, HSQC, HMBC and HSQCAD, see SI for NMR data) and two crystal structures were also obtained for peptoids **12** and **14**.

Table 1. Sequence of the Peptoid Synthesized, Purity and Mass Spectra Data for Peptoids 1-16

Peptoid	l^a	monomer sequence	% purity ^b	expected mass	observed mass
1	6	Ac- <i>Ns1tbe</i> - <i>Ns1tbe</i> - <i>Ns1tbe</i> - <i>Ns1tbe</i> - <i>Ns1tbe</i> - <i>NtBu</i> - <i>OrBu</i>	96%	934.74	935.75 [M+H] ⁺
2	6	Ac- <i>Ns1tbe</i> - <i>Ns1tbe</i> - <i>Ns1tbe</i> - <i>Ns1tbe</i> - <i>NtBu</i> - <i>Ns1tbe</i> - <i>OrBu</i>	>95%	934.74	935.75 [M+H] ⁺
3	6	Ac- <i>Ns1tbe</i> - <i>Ns1tbe</i> - <i>Ns1tbe</i> - <i>NtBu</i> - <i>Ns1tbe</i> - <i>Ns1tbe</i> - <i>OrBu</i>	97%	934.74	935.75 [M+H] ⁺
4	6	Ac- <i>Ns1tbe</i> - <i>Ns1tbe</i> - <i>NtBu</i> - <i>Ns1tbe</i> - <i>Ns1tbe</i> - <i>Ns1tbe</i> - <i>OrBu</i>	96%	934.74	935.74 [M+H] ⁺
5	6	Ac- <i>Ns1tbe</i> - <i>NtBu</i> - <i>Ns1tbe</i> - <i>Ns1tbe</i> - <i>Ns1tbe</i> - <i>Ns1tbe</i> - <i>OrBu</i>	98%	934.74	957.73 [M+Na] ⁺
6	6	Ac- <i>NtBu</i> - <i>Ns1tbe</i> - <i>Ns1tbe</i> - <i>Ns1tbe</i> - <i>Ns1tbe</i> - <i>Ns1tbe</i> - <i>OrBu</i>	98%	934.74	935.75 [M+H] ⁺
7	6	Ac- <i>NtBu</i> - <i>Ns1tbe</i> - <i>NtBu</i> - <i>Ns1tbe</i> - <i>NtBu</i> - <i>Ns1tbe</i> - <i>OBn</i>	98%	912.66	913.67 [M+H] ⁺
8	6	Ac- <i>NtBu</i> - <i>Ns1tbe</i> - <i>NtBu</i> - <i>Ns1tbe</i> - <i>NtBu</i> - <i>Ns1tbe</i> - <i>OH</i>	96%	822.62	823.62 [M+H] ⁺
9	6	Ac- <i>NtBu</i> - <i>NtBu</i> - <i>Ns1tbe</i> - <i>Ns1tbe</i> - <i>NtBu</i> - <i>NtBu</i> - <i>OrBu</i>	>99%	850.65	851.65 [M+H] ⁺
10	7	Ac- <i>NtBu</i> - <i>NtBu</i> - <i>Ns1tbe</i> - <i>Ns1tbe</i> - <i>Ns1tbe</i> - <i>NtBu</i> - <i>NtBu</i> - <i>OrBu</i>	>97%	991.77	1014.75 [M+Na] ⁺
11	9	Ac- <i>NtBu</i> - <i>NtBu</i> - <i>NtBu</i> - <i>Ns1tbe</i> - <i>Ns1tbe</i> - <i>Ns1tbe</i> - <i>NtBu</i> - <i>NtBu</i> - <i>NtBu</i> - <i>OrBu</i>	95%	1217.93	1218.93 [M+H] ⁺
12	3	Ac- <i>NtBu</i> - <i>Ns1tbe</i> - <i>Ns1tbe</i> - <i>OrBu</i>	>99%	511.40	512.40 [M+H] ⁺
13	4	Ac- <i>Ns1tbe</i> - <i>NtBu</i> - <i>Ns1tbe</i> - <i>Ns1tbe</i> - <i>OrBu</i>	99%	652.51	653.52 [M+H] ⁺
14	5	Ac- <i>Ns1tbe</i> - <i>Ns1tbe</i> - <i>NtBu</i> - <i>Ns1tbe</i> - <i>Ns1tbe</i> - <i>OrBu</i>	98%	793.63	794.63 [M+H] ⁺
15	6	Ac- <i>NtBu</i> - <i>Ns1tbe</i> - <i>Ns1tbe</i> - <i>NtBu</i> - <i>Ns1tbe</i> - <i>Ns1tbe</i> - <i>OrBu</i>	>98%	906.71	907.72 [M+H] ⁺
16	9	Ac- <i>NtBu</i> - <i>Ns1tbe</i> - <i>Ns1tbe</i> - <i>NtBu</i> - <i>Ns1tbe</i> - <i>Ns1tbe</i> - <i>NtBu</i> - <i>Ns1tbe</i> - <i>Ns1tbe</i> - <i>OrBu</i>	>99%	1302.03	1303.03 [M+H] ⁺

^aNumber of residues

^bDetermined by integration of the HPLC UV trace at 214 nm.

X-ray Studies for Peptoids **12** and **14**.

Crystals of trimer **12** and pentamer **14** suitable for X-ray crystallography were obtained by slow evaporation in ethyl acetate (Figure 2) and crystals of **12** were solved in the P1 space group and crystals of **14** were solved in the P2₁2₁2₁ space group. The high resolution structures of trimer **12** and pentamer **14** complement the previously reported X-ray structures for *NtBu* (dimer, trimer and pentamer) and *Ns1tbe* (pentamer) homo-oligomers, and mixed *NtBu*/*Ns1tbe* (compound **B**, Table 3) oligomers.^{16,29,30} The dihedral angles for **12** and **14** are characteristic of the PPI-helical fold, primarily the ω values which are indicative of all-*cis* patterns. Some of the amide bonds display a significant distortion from planarity, especially the amide bond between residues 3 and 4 of **14** ($\omega = -24.7$). The discrepancy between the ϕ values of the *NtBu* (≈ -90) and *Ns1tbe*

monomers (≈ -70) has already been noted (see Figure 1).¹⁶ The φ torsion angle at the C-terminus of **14** is positive (+80.7), the opposite of what is expected from the *S* configuration. This may be due to packing considerations together with the greater flexibility of the C-termini of peptoid chains. The difference of side-chains χ_1 dihedral angles between the two types of monomers, has also been noted earlier (see Figure 1).¹⁶

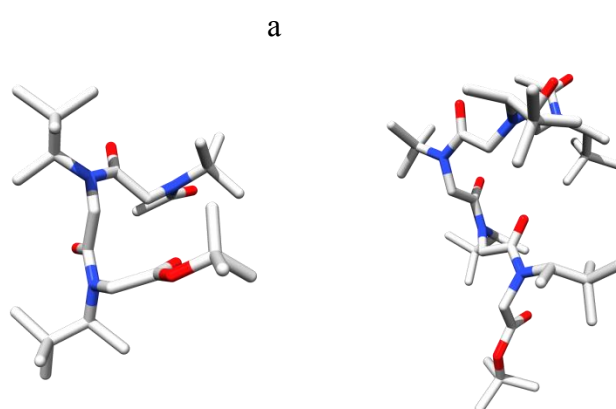
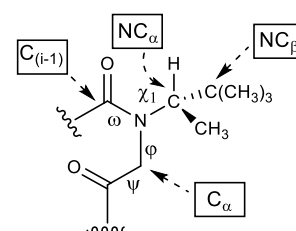


Figure 2. High resolution structures of peptoid trimer **12** (a) and pentamer **14** (b) as determined by X-ray crystallography.

Table 2. Observed torsion angles for peptoids 12 and 14 as determined by X-ray crystallography

Peptoid	residue	ω	φ	ψ	χ_1
12	<i>Nt</i> Bu	11.6	-92.7	-165.6	-81.0
	<i>Ns1tbe</i>	-2.1	-67.1	174.2	-101.0
	<i>Ns1tbe</i>	-5.3	-69.1	-	-98.3
14	<i>Ns1tbe</i>	-15.6	-69.5	-178.9	-100.4
	<i>Ns1tbe</i>	-11.3	-71.7	173.4	-100.0
	<i>Nt</i> Bu	-13.0	-88.5	-178.2	-60.6
	<i>Ns1tbe</i>	-24.7	-71.2	-161.7	-105.1
	<i>Ns1tbe</i>	-3.02	80.7	-	-102.8



Dihedral angles definition: ω [$C\alpha(i-1)$; $C(i-1)$; N ; $C\alpha$], φ [$C(i-1)$; N ; $C\alpha$; C], ψ [N ; $C\alpha$; C ; $N(i+1)$], χ_1 [$C(i-1)$; N ; $NC\alpha$; $NC\beta$]

Overall backbone amide $K_{cis/trans}$ values. Conformational control of a peptoid chain rests first on the individual control of its amide bonds geometry, i.e. *cis* or *trans*. The PPI-like conformation involves a continuous succession of *cis*-amide bonds. It has been established that *Nt*Bu

monomers do form *cis*-amide bonds with their preceding residue, independently of the oligomer length. We therefore focussed on the *cis/trans* isomerization of the *Ns1tbe* residues with their preceding units. For that purpose, we have looked at the NC α methyne protons of the *Nstbe* residues, which display separate NMR chemical shifts in the *cis* and *trans* conformations (determined previously by COSY and NOESY NMR experiments).¹⁶ The methyne proton of the *Ns1tbe* is deshielded by approximately 1.0 ppm in the *cis* conformation (\approx 4.6 ppm) relative to the *trans* (\approx 3.6 ppm), in accordance with reported data on both aromatic and aliphatic side-chains.^{15,26,28,42} The overall $K_{cis/trans}$ values were determined in deuterated chloroform, acetonitrile, and methanol (for some representative compounds), by integration of the *cis* and *trans* methyne proton-carbon correlations of 2D-NMR HSQCAD experiments (Table 3). From this first series of values corresponding to the overall $K_{cis/trans}$ for the amide bonds between the *Ns1tbe* residues and their preceding residues, a second series of $K_{cis/trans}$ values was calculated by including the *NtBu*-based amide linkages. For each sequence, the weighted average $K_{cis/trans}$ were estimated taking a $K_{cis/trans}$ of 32 for the *NtBu* monomers (97% of *cis*).

Table 3. Peptoid Structure and Overall $K_{cis/trans}$ Values as determined by integration of HSQCAD NMR spectra in $CDCl_3$ and CD_3CN

peptoid	l^a	% chiral side chains	Monomer sequence ^b	weighted average of $K_{cis/trans}$ ($Ns1tbe$ residues) ^c			weighted average of $K_{cis/trans}$ (all residues) ^d		
				$CDCl_3$	CD_3CN	CD_3OD	$CDCl_3$	CD_3CN	CD_3OD
1	6	83	c-c-c-c-c-a	> 49.0 ^e	> 49.0 ^e	> 49.0 ^e	> 49	> 49	> 49.0
2	6	83	c-c-c-c-a-c	11.9	7.7		> 15.2	> 11.7	
3	6	83	c-c-c-a-c-c	11.2	5.9		> 14.6	> 10.2	
4	6	83	c-c-a-c-c-c	16.2	6.3		> 18.8	> 10.5	
5	6	83	c-a-c-c-c-c	11.0	7.8		> 14.5	> 11.8	
6	6	83	a-c-c-c-c-c	18.0	9.7	29.5	> 20.3	> 13.4	32.7
7	6	50	a-c-a-c-a-c	2.0	1.7		> 17.0	> 16.8	
8	6	50	a-c-a-c-a-c	-	-		-	-	
A ¹⁶	6	66	a-c-c-c-c-a	> 19.0	> 19.0		> 23.3	> 23.3	
B ¹⁶	8	50	a-a-c-c-c-c-a-a	> 19.0	> 19.0		> 25.5	> 25.5	
9	6	33	a-a-c-c-a-a	23.5	19.5	33.3	> 29.1	> 27.8	43.7
10	7	43	a-a-c-c-c-a-a	> 49.0 ^e	32.8		> 49	> 42.0	
11	9	33	a-a-a-c-c-c-a-a-a	> 49.0 ^e	> 49.0		> 49.0	> 49.0	
12	3	66	a-c-c	2.4	-		> 12.2	-	
13	4	75	c-a-c-c	2.0	-		> 9.5	-	
14	5	80	c-c-a-c-c	3.6	7.7		> 9.3	> 12.5	
15	6	66	a-c-c-a-c-c	12.3	6.8	19.6	> 18.8	> 15.2	29.4
16	9	66	a-c-c-a-c-c-a-c-c	4.2	15.0	15.9	> 13.4	> 20.6	26.9

^aNumber of residues

^bThe achiral *NtBu* monomers are represented by the letter “a” and the chiral *Ns1tbe* by “c”

^cDetermined for the amide bonds between *Ns1tbe* residues and their preceding residues

^dDetermined for all the residues, considering that the *NtBu* monomers form exclusively *cis*-amide bonds with their preceding (*i-1*) residues. Calculation was made with $K_{cis/trans} = 32$ for the *NtBu* monomers (97% of *cis*)

^eTrans rotamers were not detected.

Acetonitrile has been commonly used in structural studies of peptoids, notably those with α -chiral aromatic side chains which were found to adopt the all-*cis* PPI helix conformation. Acetonitrile is recognized to minimize interamide $n \rightarrow \pi^*_{C=O}$ interactions within peptoid, thereby destabilizing the *trans* amide conformation.²⁶ Furthermore, determination of the *cis/trans* ratio of the *N*-terminal acetamide of diamide peptoid model systems, expected to reproduce the behavior of larger peptoid oligomers, indicates that the fraction of *cis* isomer is generally higher in acetonitrile than in methanol or chloroform, at least for uncharged side chains.²⁶ This trend is not verified for the peptoids **1-16** (Table 3). Indeed, with the exception of peptoids **14** and **16**, the fraction of *cis* isomer is higher in non-polar $CDCl_3$ than in CD_3CN , and is even higher in d_4 -methanol, as seen from the $^{CD_3OD}K_{cis/trans}$ determined for the representative compounds **1**, **6**, **9**, **15** and **16** for which the *trans* rotamers are completely or largely suppressed. Also of note from the comparison of the overall $K_{cis/trans}$ for compounds **1-6** is that the positioning of a single *cis*-enforcing *NtBu* monomer at the carboxy terminus proves exceptionally efficient to suppress the

trans-amide rotamers. This is consistent with the finding that the carboxy terminus of the PPI peptoid helix is structurally less stable than the amino terminus.³⁶ Although the *cis/trans* isomerization of the backbone tertiary amides is totally suppressed in the case of peptoid **1**, its ¹H NMR spectrum (CDCl₃) showed a very small amount of residual conformational heterogeneity, evidenced for example on the CO₂*t*Bu resonance, which is no longer present in *d*₄-methanol. There is also evidence that the peptoids containing a central chiral segment of 2 to 4 *Ns1tbe* consecutive residues, surrounded by *Nt*Bu residues display the higher overall $K_{cis/trans}$ (**A**, **B**, **9-11**). In contrast, the incorporation of *Nt*Bu monomers every two *Ns1tbe* residues (**12-16**) does not ensure the complete suppression of the peptoid amide *cis-trans* rotameric isomerism.

Circular dichroism of hexamers 1-6. The CD spectra of oligomers **1-6** are shown in Figure 3. All the CD curves are well-defined and display the spectral features that are typically associated to the polyproline type I helix of peptoids substituted with aliphatic side-chains, i.e., two minima at 190 nm and 225 nm, and a positive maximum around 210 nm.¹⁴ In acetonitrile, compound **1** with the *Nt*Bu monomer positioned at the *C*-terminus displays the more intense ellipticity on a per-residue molar basis (MRE = 11 741 at 208 nm, Figure 3a and Figure S2), at a high level comparable to that of the nonamer Ac-(*Ns1tbe*)₉-*Ot*Bu (MRE = 12 673, 210 nm).¹⁶ By contrast, hexamers **5** and **6** with the *Nt*Bu residues located at the 2nd and first position of the sequence (from N to C), display lower ellipticities (MRE = 4324 for **6** at 208 nm), of the same order of magnitude as that of the homo-pentamer Ac-(*Ns1tbe*)₅-*Ot*Bu (MRE = 4967 at 208 nm).¹⁶ Compounds **2**, **3** and **4**, form a homogeneous group whose ellipticity at 208 nm (in the range 6100-6900) is intermediate those of compound **1** and **5/6**. On the whole, there appears to be a trend toward ellipticity decreasing with increasing remoteness of the *Nt*Bu monomer from the carboxy terminus. This was further verified in MeOH, in which the spectral intensity at 208 nm consistently decreases when the *Nt*Bu unit moves away from the carboxy terminus (Figure 3b and 4). The strongest CD intensity of hexamer **1** within the group of peptoids **1-6** is consistent with an all *cis*-amide backbone ($K_{cis/trans} > 49$ in deuterated chloroform, acetonitrile and methanol, Table 3). The ^{CD₃CN} $K_{cis/trans}$ values between 10.2 and 13.4 for hexamers **2-6** are indicative of a remaining backbone amide conformational heterogeneity (*trans* rotamers populated at 7-9%), comparable to that of the peptoid hexamer Ac-(*Ns1tbe*)₆-*Ot*Bu (^{CD₃CN} $K_{cis/trans}$ = 10.4).¹⁶ An increase of ellipticity (compound **2**) and a decrease (compound **6**) are observed by switching the solvent from acetonitrile to methanol, but more generally, this first series of peptoids is not much affected by solvent polarity, which is consistent with the fact that the conformation is primarily governed by steric interactions.¹⁵ This is in contrast with the CD spectra of the *Ns1tbe*

homooligomers which were decreased in methanol relative to those in acetonitrile.¹⁶ This suggests that the presence of a single bulky *Nt*Bu residue within the peptoid sequence may already have a positive effect on the conformational stability.

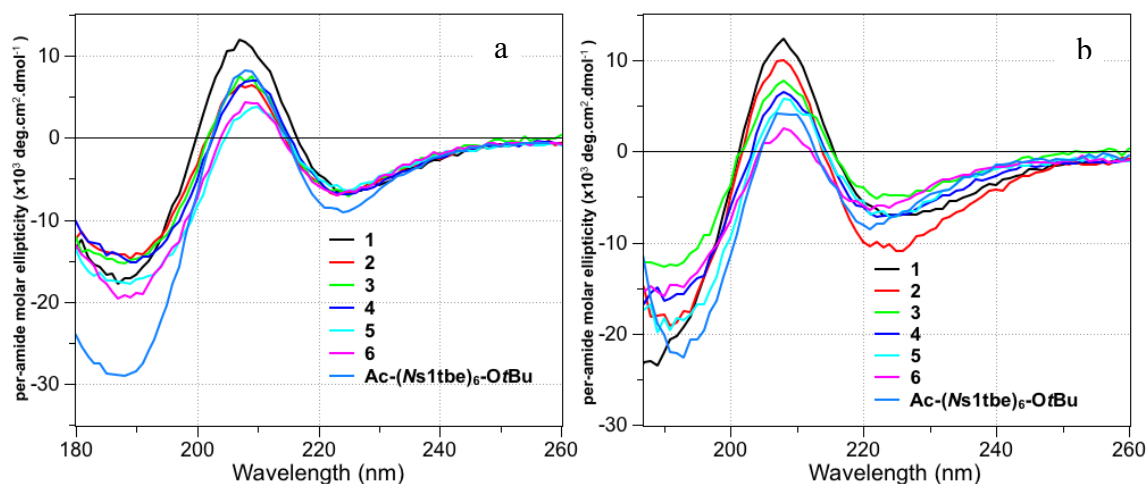


Figure 3. CD spectra of hexamers **1-6** and reference compound Ac-(Ns1tbe)₆ in acetonitrile (a) and methanol (b).

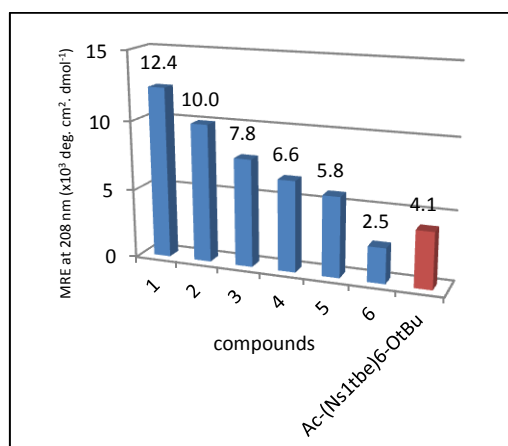


Figure 4. MRE values of hexamers **1-6** and reference compound Ac-(Ns1tbe)₆ at 208 nm in MeOH

Of note, is the significant difference between the intensity of the negative band at 190 nm between the homo-oligomer Ac-(Ns1tbe)₆-OtBu and the hexamers **1-6**. For hexamers **1-6**, the negative band at 190 nm also tends to increase with the decrease of the positive band at 210 nm. Interestingly, the CD curves of hexamers **1** (c-c-c-c-c-a) and **A** (a-c-c-c-c-a) in acetonitrile and methanol are virtually superposable (Figure 5), which in the light of the previous results, show that within this group of peptoids, a single *Nt*Bu monomer strategically positioned at the C-terminus is sufficient to achieve a robust helical structure. Also of note is that, once a first *Nt*Bu is positioned at the C-terminus, a second mutation of a chiral *Ns*1tbe monomer by a *Nt*Bu at the N-terminus is not detrimental to peptoid helicity, albeit a decrease of the amount of chiral side-

chains from 83% (**1**) to 66% (**A**). “Ends effects” have been observed previously in the study of peptoids and retropeptoids composed of aromatic chiral and achiral monomers.³⁶ It has been shown, for example, that placing a bulky chiral *Ntpe* monomer on the carboxy terminus rather than on the amino terminus dramatically increased CD intensity.

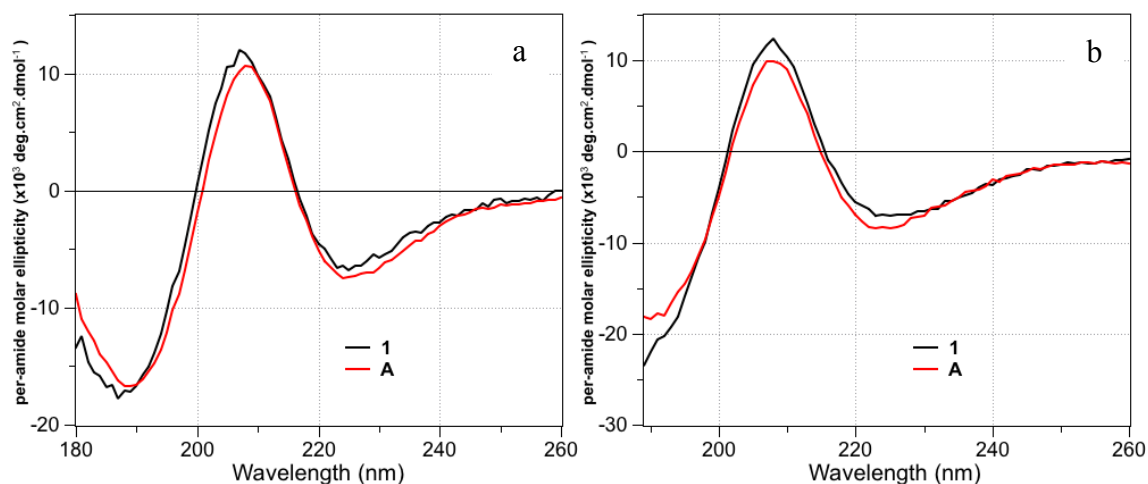


Figure 5. CD spectra of hexamers **1** and **A** in acetonitrile (a) and methanol (b).

Circular dichroism of hexamers 7-11.

The CD spectra of the alternated (*NtBu-Ns1tbe*)₃ hexamer **7** and its corresponding free carboxy acid **8** are shown in figures S3-S5. The hexamer **7** is better structured in methanol than in acetonitrile with a MRE value at 208 nm in methanol nearly twice that in acetonitrile. The CD spectrum of **7** in MeOH is close to those of hexamers **A** and **15** in shape and intensity (Figure S4). In contrast, a significant decrease of helical fold was observed for the free acid hexamer **8**, notably in acetonitrile and acetonitrile/aqueous buffer solutions, as compared to the ellipticity in methanol (Figure S5).

All three compounds **9-11** are characterized by a central chiral portion (2 or 3 *Ns1tbe* residues), flanked on both ends by achiral segments of same length (2 or 3 *NtBu* residues). Their CD curves were compared to those of the reference compounds **A** and **B** (Figure 6). The CD curves of peptoids **9-11** in acetonitrile show a profile similar to those of compounds **A** and **B**, albeit with reduced intensities of the maxima. The positive band of peptoids **9** and **11** (211 nm) is blue shifted by 3 nm relative to that of peptoid **A** (208 nm), which seems to be in line with their smaller chiral content. (33% for **9** and **11** vs 66% for **A**, Tables 2). The decline in the ellipticity of peptoids **9-11** relative to **A** in acetonitrile, as estimated in the region of the spectra at around 210 nm, is more pronounced for the nonamer **11** (- 43%), than for the heptamer **10** (- 31%) and the hexamer **9** (- 26%). We find that in methanol; more intense CD spectra are obtained,

indicating a more robust helical fold. The oligomers **9** and **11** display the strongest intensities ($MRE_{209\text{ nm}} > 12\ 000$), after the octamer **B** ($MRE_{209\text{ nm}} = 15\ 000$). It is premature to establish a relationship between the monomer composition of this sub-family of peptoids (**9-11**, **A** and **B**) and their conformational properties, but some notable observations can be made. In both solvents, the intensity of the negative band at 190 nm increases with the increase of proportion of *s*1tbe chiral side-chains (SI, Table S2), suggesting a contribution from coupling interactions between the *s*1tbe side chains and backbone groups. Also, the per-residue molar ellipticity of peptoid **9** (a-a-c-c-a-a) is remarkable, considering its short length and low percentage of chiral side chains (33%). The MRE intensity of peptoid **9** at 208 nm is at the same level as that of hexamer **1**, which has 83% of chiral side-chains (SI, Figure S6). In addition, the CD spectrum of hexamer **9** in methanol has comparable shape and intensity to that of the nonamer **11** (a-a-a-c-c-a-a-a), also composed of only 33% of chiral residues. This is the first time that peptoids composed of just one-third α -chiral side chains give a stronger CD signal than their parent peptoid comprising only chiral side chains.

The few compounds studied here owning the generic sequence $(a)_x(c)_y(a)_x$ with (a) and (c) corresponding to the achiral *N*tBu and chiral *N*s1tbe monomers, respectively, show that this design principle is advantageous to achieve a stable helical folding with a low content of chiral side chains. The central segment in the oligomers studied is able to transfer its chirality with great efficacy to both ends of the oligomers.

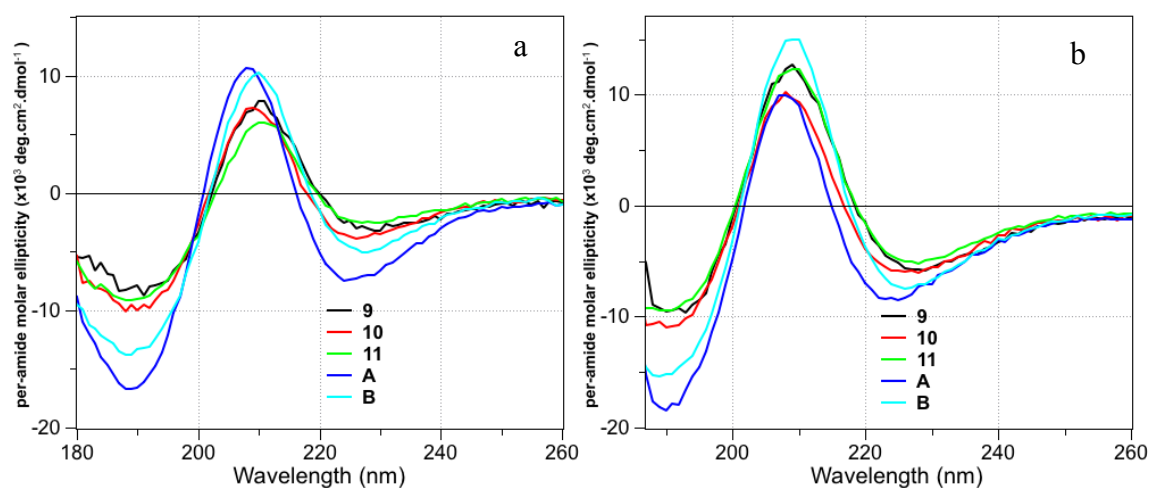


Figure 6. CD spectra of peptoids **9-11**, **A** and **B** in acetonitrile (a) and methanol (b).

Circular dichroism of peptoids **12-16**.

Characterization of peptoids **12-16** by CD shows that the minimum chain length to obtain the characteristic helix-like profile is the pentamer length (**14**) (Figure 7). Indeed, trimers **12** and tetramers **13** show no helical structure by CD (Figure 7 and 8). The CD spectra of pentamer **14**

and hexamer **15** show that the signal intensity increases with increasing the length by one residue. In contrast, comparison of spectra for hexamer **15** (a-c-c)₂ and nonamer **16** (a-c-c)₃ in acetonitrile and methanol shows that the intensity at ≈ 210 nm does not increase with the oligomer length. The positive band of **16** is even slightly diminished (and red-shifted by 3 nm) relative to **15** (Figure 7), despite the fact that the overall backbone amide cis:trans ratio is higher for **16** ($^{CD_3CN}K_{cis/trans} = 20.6$) than for **15** ($^{CD_3CN}K_{cis/trans} = 15.2$). These observations suggest that the (a-c-c)_n sequence design does not allow for an optimal propagation of the chiral secondary structure.

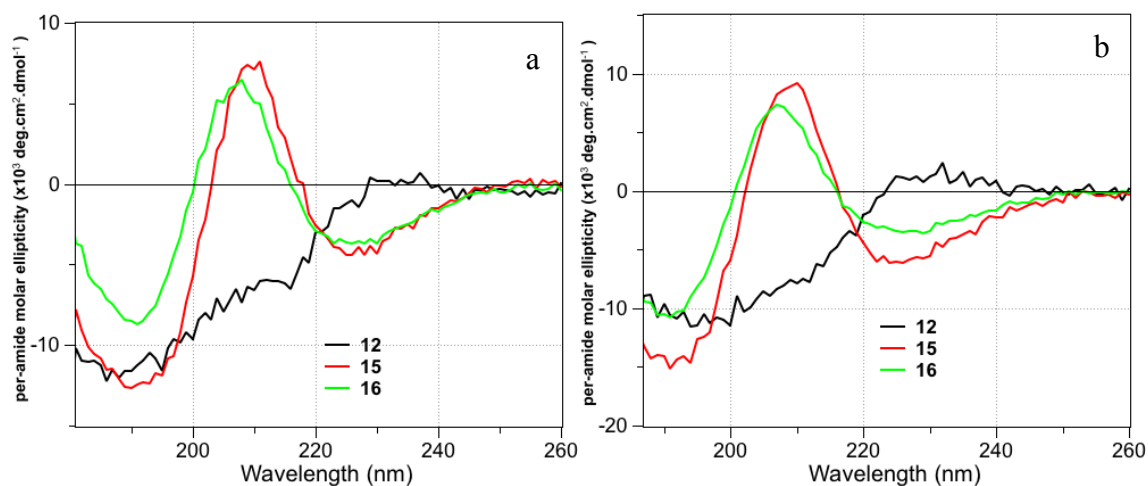


Figure 7. CD spectra of peptoids **12**, **15** and **16** corresponding to (a-c-c)_n ($n = 1, 2, 3$), in acetonitrile (a) and methanol (b).

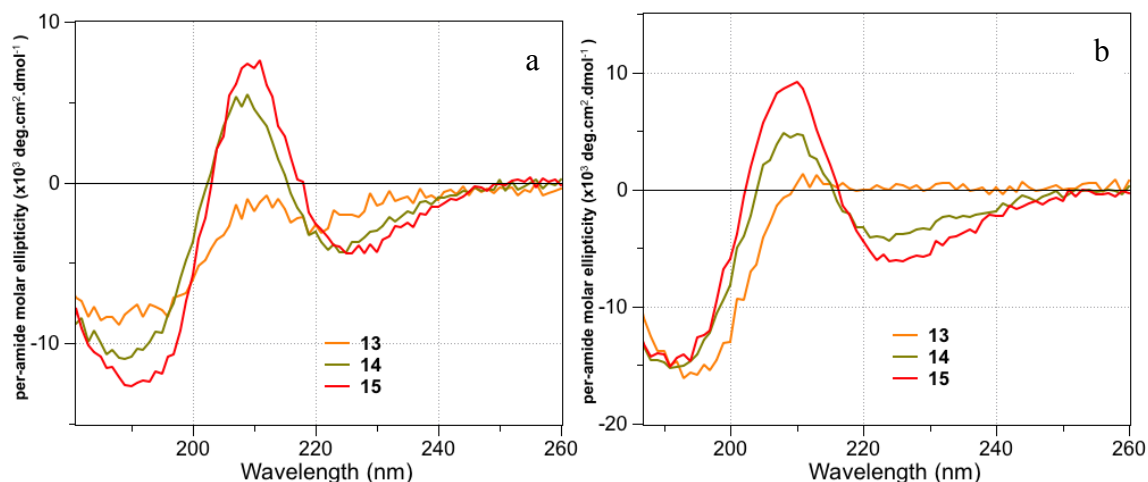


Figure 8. CD spectra of peptoids **13** (c-a-c-c), **14** (c-c-a-c-c) and **15** (a-c-c-a-c-c), in acetonitrile (a) and methanol (b).

Temperature study of compound **16**

Previously, we demonstrated the thermal conformational stability of the PPI-like helix of the homo-nonamer Ac-(Ns1tbe)₉-OtBu.¹⁶ In contrast, the degree of helical fold significantly decreased upon heating the solution of the nonamer **16**, AcO-(NtBu-Ns1tbe-Ns1tbe)₃-OtBu, in

acetonitrile from 15 to 75 °C, demonstrating the lesser thermal stability of *Ns1tbe*-based peptoid sequences incorporating *NtBu* monomers at every two residues (SI, Figure S7). Nevertheless, when the sample was cooled back to 15 °C, reversibility took place, giving back a CD spectrum of same shape and intensity than at start (SI, Figure S8). The helical folding sensitivity of the nonamer **16** to an increase of temperature was also examined by NMR by measuring the average $K_{cis/trans}$ for the *Ns1tbe* units within the peptoid backbone at various temperatures (CD₃CN, 15-75 °C) (Table S3). We observed a gradually decrease in $^{AVG}K_{cis/trans}$ with increasing the temperature, going from a value of 18.3 at 15 °C (95% of *cis* rotamer) to 2.1 at 75 °C (68% of *cis* rotamer). We therefore confirm that the decrease of helical folding upon elevating the temperature can be essentially ascribed to the increase of *cis/trans* rotameric heterogeneity.

In summary, we investigated the effect of site-specific placement of *NtBu cis*-inducer monomer on the helical secondary structure of *Ns1tbe*-based sequences. The synthesized oligomers **1-16** comprising exclusively aliphatic side-chains, chain lengths between 3 and 9 residues, of which ten are hexamers, and percentages of chiral monomers ranging from 33 to 83% were analyzed by NMR, CD spectroscopy and X-ray diffraction for two of them. The degree of helical fold was estimated by CD at around 210 nm which corresponds to the more relevant signal for the PPI-like helix of peptoids carrying aliphatic side-chains. Switching the solvent from acetonitrile to methanol increased the fraction of *cis* isomer as seen from the NMR of the representative peptoids **1**, **6**, **9**, **15** and **16**. This observation is commensurate with the CD spectra of the peptoids in methanol which are either identical or greater in intensity as compared to those observed in acetonitrile. At this time no correlation can be found between the intensity of the negative band at 190 nm and the monomer composition of the peptoids. It is noteworthy that the CD spectrum of the short length tetramer **13** only displays this negative band around 190 nm. A single mutation of each of the six *Ns1tbe* residues of homo-oligomer (*Ns1tbe*)₆ to *NtBu* residue (hexamers **1-6**) was used to probe the influence of the positioning of a single achiral *tBu* side chain on the helical structure. We show that a single *NtBu* monomer at the carboxy terminus enables to completely suppress the backbone *trans*-amide rotamers and consequently reinforce the helical fold of peptoid hexamers. This finding is consistent with the fact that the carboxy terminus of the peptoid helix is recognized to be less structurally stable than the amino terminus.³⁶ We anticipate that this favorable C-terminal stabilizing “end effect” might also operate in longer peptoids, including oligomers carrying aromatic side chains. Of the ten hexamer sequences studied, peptoid **9** consisting of two central *Ns1tbe* residues flanked at both ends by two *NtBu* residues revealed a remarkable helical folding, especially in methanol, in view

of its rather short length and low content of chiral sides chains (33%). Overall, the sequence design consisting of a central chiral segment flanked by achiral parts (**9-11**) permits an efficient helical chirality transfer to the peptoid extremities. In contrast, the incorporation of *Nt*Bu monomers every two residues, thus forming an achiral helix face, results in a slight decrease of helicity. Our finding will be useful to reinforce the stability of organosoluble peptoid helices aimed at interacting with a biological hydrophobic environment such as phospholipidic membranes. Work is now in progress to extend the scope of our finding to peptoids incorporating chiral aromatic monomers, hydrosoluble monomers and functional monomers.

EXPERIMENTAL SECTION

General methods. THF, CH₂Cl₂ were dried over aluminum oxide via a solvent purification system. EtOAc, CH₂Cl₂, cyclohexane, and MeOH for column chromatography were obtained from commercial sources and were used as received. All other solvents and chemicals obtained from commercial sources were used as received. Melting points were determined on a Stuart Scientific SMP3 microscope apparatus and are uncorrected. NMR spectra were recorded on a 400 MHz Bruker Avance III HD spectrometer or a 500 MHz Bruker AC-500 spectrometer. Chemical shifts are referenced to the residual solvent peak and *J* values are given in hertz. The following multiplicity abbreviations are used: (s) singlet, (ls) large singlet, (d) doublet, (t) triplet, (q) quartet, (m) massif, and (br) broad. Where applicable, assignments were based on COSY, HMBC, HSQC, and ¹³C experiments. TLC was performed on Merck TLC aluminum sheets, silicagel 60, F₂₅₄. Progression of reactions was, when applicable, followed by TLC. Visualizing of spots was effected with UV-light and/or vanillin in EtOH/H₂SO₄. Flash chromatography was performed with Merck silica gel 60, 40–63 μm. HRMS was recorded on a Micromass Q-ToF Micro (3000 V) apparatus or a Q Exactive Quadrupole-Orbitrap Mass Spectrometer. LC–MS was recorded a Q Exactive Quadrupole-Orbitrap mass spectrometer coupled to a UPLC Ultimate 3000 (Kinetex EVO C18; 1.7 μm; 100 mm × 2.1 mm column with a flow rate of 0.45 mL min⁻¹ with the following gradient: a linear gradient of solvent B from 5% to 95% over 7.5 min (solvent A = H₂O + 0.1% formic acid, solvent B = acetonitrile + 0.1% formic acid) equipped with a DAD UV/vis 3000 RS detector. HPLC analysis was performed on a Dionex instrument equipped with an Uptisphere (ODB, 5 μm, 120 Å, 4.6 × 250 mm) and a Dionex UVD 340 detector. X-ray data were collected at 100 K with an Oxford Diffraction Xcalibur 2 diffractometer equipped with a copper microsource ($\lambda = 1.5418 \text{ \AA}$).

NMR experiments. A Bruker Avance III HD 500 spectrometer operating at 500.13 MHz for ¹H and 125.77 MHz for ¹³C with a 5 mm pulsed-field z-gradient TXI probe was used. For each

sample, the probe was carefully tuned, and all normal and adiabatic pulses were well calibrated. For each 2D heteronuclear $^1\text{H}/^{13}\text{C}$ HSQCAD (Bruker sequence: hsqcedetgpcisp2.3) experiments were performed with quadrature phase detection in dimensions, using Echo-Antiecho detection mode in the indirect one. For each 768 increments in the indirect dimension, 2K data points were collected and 8 transients were accumulated in the direct dimension. Adiabatic ^{13}C decoupling (Bruker sequence : bi_p5m4sp_4sp.2) was performed during acquisition. The spectral widths (SW) were fixed to 8 ppm for ^1H and to 165 ppm for ^{13}C . A $\pi/2$ shifted square sine-bell function was applied in the two dimensions before Fourier transformation. Spectra were acquired and treated with Bruker Topspin version 3.5p15 and referenced to solvent. All NMR spectra were recorded at 298K.

Circular Dichroism Spectroscopy in the far-UV range. Peptoid stock solutions were prepared by dissolving at least 2 mg of each peptoid, weighed using a high-precision balance (Sartorius), in spectroscopic grade acetonitrile or methanol. The stock solutions then were diluted with spectroscopic grade solvent to the concentration of 500 μM . CD experiments were carried out in a Chirascan-plus spectropolarimeter equipped with a Peltier system (Applied Photophysics Ltd, Surrey, UK). CD spectra were obtained in a flat quartz cell (path length 0.01 cm) at 293°K using a scan rate of 0.5 nm/sec, in the far-UV range (180 to 260 nm) and are the average of three successive measurements. The spectrum of a solvent blank was subtracted from the raw CD data, and the resulting data were expressed in terms of per-amide molar ellipticity ($\text{deg}\cdot\text{cm}^2\cdot\text{dmol}^{-1}$), as calculated per mole of amide groups present and normalized by the molar concentration of peptoid.

General procedure for the solution-phase synthesis of peptoids 1-16 by the submonomer protocol. *tert*-Butyl bromoacetate was used as starting material for all synthesized compounds with the exception of the synthesis of hexamers **7** and **8** for which benzyl bromoacetate was used. The commercially available primary amines *tert*-butylamine or the (2*S*)-3,3-dimethylbutan-2-amine (*sIthe* amine) were employed for the substitution steps. The bromoacetamide compounds were purified by flash silica gel chromatography prior to their reaction with the submonomer primary amine building blocks

General procedure A: Submonomer bromine atom substitution with primary amines. To a solution of *tert*-butyl bromoacetate (or benzyl bromoacetate for the synthesis of peptoid **7**) or crude bromoacetyl amide (1.0 equiv, 0.2 M) in EtOAc or THF at rt was added Et_3N (2.0 equiv.) followed by the chosen primary amine (4.0 equiv.). After stirring overnight at room temperature, the resulting mixture was diluted with EtOAc (10mL per mmol of starting material) and filtered, washing the solids with EtOAc. The filtrate was then concentrated under reduced pressure.

EtOAc was added to the residue which was then concentrated under reduced pressure. This was repeated twice and the residue was dried *in vacuo*, yielding the desired crude secondary amine which was used in the next step without further purification.

General procedure B: Submonomer bromoacetylation. To a solution of the crude secondary amine (1.0 equiv, 0.2 M) in dry THF (or EtOAc) at -10°C under argon was added Et₃N (1.2 equiv.) and then bromoacetyl bromide (1.05 equiv.). After stirring for 1 h at -10°C the resulting mixture was diluted with EtOAc (10 mL per mmol of starting material) and the salts were filtered, washing the solid with EtOAc. The filtrate was then concentrated *in vacuo*, yielding the crude bromoacetyl amide which was purified by flash column chromatography on silica gel.

General procedure C: terminal N-acetylation. To a solution of a peptoid (1 equiv.) and Et₃N (1.4 equiv.) in dry EtOAc (0.2 M) at 0°C under Ar, was added dropwise AcCl (1.2 equiv.) and the reaction mixture was stirred overnight at room temperature. The mixture was filtered, and the solids washed with EtOAc. The filtrate was then concentrated *in vacuo*, yielding the crude N-terminal acetylated compound which was purified by flash column chromatography on silica gel.

Peptoid hexamer 1 (Ac-Ns1tbe-Ns1tbe-Ns1tbe-Ns1tbe-Ns1tbe-NtBu-OtBu). The peptoid **1** was synthesized in 12 steps from *tert*-butyl bromoacetate (390 mg, 2.0 mmol) according to procedures A and B for the submonomer elongation steps and procedure C for the final N-terminal acetylation. Peptoid **1** was isolated as a white solid after purification by flash column chromatography on silica gel. (89 mg, 0.095 mmol); $R_f = 0.54$ (100% EtOAc). m.p. 227.5-228.5 °C HRMS (TOF MS ES+) m/z calcd for C₅₂H₉₉N₆O₈ [M+H]⁺ 935.7518; found 935.7525. Analytical HPLC purity 96%.

¹H NMR (400 MHz, CDCl₃) δ (ppm): 0.82-1.06 (m, 60H, CH(CH₃)C(CH₃)₃), 1.42 (s, 9H, NtBu), 1.52 (s, 9H, CO₂tBu), 2.09 (s, 3H, COCH₃) 3.68-4.26 (m, 12H, NCH₂CO), 4.62-4.79 (m, 5H, H methyne *cis* rotamer).

Peptoid hexamer 2 (Ac-Ns1tbe-Ns1tbe-Ns1tbe-Ns1tbe-NtBu-Ns1tbe-OtBu). The peptoid **2** was synthesized in 12 steps from *tert*-butyl bromoacetate (390 mg, 2.0 mmol) according to procedures A and B for the submonomer elongation steps and procedure C for the final N-terminal acetylation. Peptoid **2** was isolated as a white solid after purification by flash column chromatography on silica gel. (350 mg, 0.374 mmol); $R_f = 0.64$ (100% EtOAc). m.p. 168.5-169.5 °C HRMS (TOF MS ES+) m/z calcd for C₅₂H₉₉N₆O₈ [M+H]⁺: 935.7518; found: 935.7524. Analytical HPLC purity 95%.

¹H NMR (400 MHz, CDCl₃) δ (ppm): 0.81-1.35 (m, 60H, CH(CH₃)C(CH₃)₃), 1.41 (s, 9H, NtBu), 1.45 (s, 3H, CO₂tBu), 1.50 (s, 6H, CO₂tBu), 2.10, (s, 3H, COCH₃), 3.61-4.44 (m, 12.37H, NCH₂CO and H methyne *trans* rotamer), 4.64-4.80 (m, 4.63H, H methyne *cis* rotamer).

Peptoid hexamer 3 (Ac-Ns1tbe-Ns1tbe-Ns1tbe-NtBu-Ns1tbe-Ns1tbe-OtBu). The peptoid **3** was synthesized in 12 steps from *tert*-butyl bromoacetate (150 mg, 0.77 mmol) according to procedures A and B for the submonomer elongation steps and procedure C for the final N-terminal acetylation. Peptoid **3** was isolated as a white solid after purification by flash column chromatography on silica gel. (72 mg, 0.077mmol); $R_f = 0.74$ (100% EtOAc). m.p. 178.5- 179.5 °C HRMS (TOF MS ES+) m/z calcd for $C_{52}H_{99}N_6O_8$ $[M+H]^+$: 935.7518; found: 935.7516. Analytical HPLC purity 97%.

1H NMR (400 MHz, $CDCl_3$) δ (ppm): 0.73-1.30 (m, 60H, $CH(CH_3)C(CH_3)_3$), 1.38 (s, 9H, NtBu), 1.42 (s, 3H, CO_2tBu), 1.52 (s, 6H, CO_2tBu), 2.05-2.15 (m, 3H, $COCH_3$), 3.46-4.26 (m, 12.56H, NCH_2CO and H methyne *trans* rotamer), 4.61 -4.81 (m, 4.44H, H methyne *cis* rotamer).

Peptoid hexamer 4 (Ac-Ns1tbe-Ns1tbe-NtBu-Ns1tbe-Ns1tbe-Ns1tbe-OtBu). The peptoid **4** was synthesized in 12 steps from *tert*-butyl bromoacetate (164 mg, 0.84 mmol) according to procedures A and B for the submonomer elongation steps and procedure C for the final N-terminal acetylation. Peptoid **4** was isolated as white solid after purification by flash column chromatography on silica gel. (44 mg, 0.047mmol); $R_f = 0.60$ (100% EtOAc). m.p. 140.5-141.5 °C; HRMS (TOF MS ES+) m/z calcd for $C_{52}H_{99}N_6O_8$ $[M+H]^+$: 935.7518; found: 935.7495. Analytical HPLC purity 96%.

1H NMR (400 MHz, $CDCl_3$) δ (ppm): 0.81-1.10 (m, 60H, $CH(CH_3)C(CH_3)_3$), 1.41 (s, 9H, NtBu), 1.46 (s, 2.2H, CO_2tBu) 1.51 (s, 6.8H, CO_2tBu), 2.02 (s, 2.34H, $COCH_3$), 2.05, (s, 0.25H, $COCH_3$) 2.08 (s, 0.41H, $COCH_3$), 3.61-4.44 (m, 12.54H, NCH_2CO and H methyne *trans* rotamer), 4.64-4.80 (m, 4.46H, H methyne *cis* rotamer).

Peptoid hexamer 5 (Ac-Ns1tbe-NtBu-Ns1tbe-Ns1tbe-Ns1tbe-Ns1tbe-OtBu). The peptoid **5** was synthesized in 12 steps from *tert*-butyl bromoacetate (134 mg, 0.68 mmol) according to procedures A and B for the submonomer elongation steps and procedure C for the final N-terminal acetylation. Peptoid **5** was isolated as a white solid after purification by flash column chromatography on silica gel. (142 mg, 0.15 mmol); $R_f = 0.70$ (EtOAc). m.p. 160.1-160.5 °C HRMS (TOF MS ES+) m/z calcd for $C_{52}H_{98}N_6O_8Na$ $[M+Na]^+$: 957.7339; found: 957.7305. Analytical HPLC purity 98%.

1H NMR (400 MHz, $CDCl_3$) δ (ppm): 0.81-1.08 (m, 59.2H, $CH(CH_3)C(CH_3)_3$), 1.33 (d, $J = 7.3$ Hz, 0.8H, $CH(CH_3)C(CH_3)_3$ *trans* rotamer), 1.39 (s, 2.5H, CO_2tBu), 1.42 (s, 9H, NtBu), 1.51 (s, 6.5H, CO_2tBu), 1.98-2.22 (3H, $COCH_3$), 3.5-4.37 (m, 12.54H, NCH_2CO and H methyne *trans* rotamer), 4.50-4.90 (m, 4.46H, H methyne *cis* rotamer).

Peptoid hexamer 6 (Ac-*Nt*Bu-*Ns*1tbe-*Ns*1tbe-*Ns*1tbe-*Ns*1tbe-*Ns*1tbe-*Ot*Bu). The peptoid **6** was synthesized in 12 steps from *tert*-butyl bromoacetate (97 mg, 0.50 mmol) according to procedures A and B for the submonomer elongation steps and procedure C for the final N-terminal acetylation. Peptoid **6** was isolated as a solid after purification by flash column chromatography on silica gel. (149 mg, 0.16 mmol); $R_f = 0.70$ (EtOAc). m.p. 148.2-148.6 °C HRMS (TOF MS ES+) m/z calcd for $C_{52}H_{99}N_6O_8$ $[M+H]^+$: 935.7518; found: 935.7491. Analytical HPLC purity 98%.

1H NMR (400 MHz, $CDCl_3$) δ (ppm): 0.82-1.08 (m, 59.2H, $CH(CH_3)C(CH_3)_3$ and $CH(CH_3)C(CH_3)_3$ *cis* rotamer), 1.33 (d, $J = 6.8$ Hz, 0.8H, $CH(CH_3)C(CH_3)_3$ *trans* rotamer), 1.40-1.54 (m, 18H, *Nt*Bu and CO_2t Bu), 1.98-2.21 (m, 3H, $COCH_3$), 3.46-4.28 (m, 12.50H, NCH_2CO and H methyne *trans* rotamer), 4.62-4.79 (m, 4.50H, H methyne *cis* rotamer).

Peptoid hexamer 7 (Ac-*Nt*Bu-*Ns*1tbe-*Nt*Bu -*Ns*1tbe-*Nt*Bu-*Ns*1tbe-*OBn*). The peptoid **7** was synthesized in 12 steps from benzyl bromoacetate (452 mg, 1.97 mmol) according to procedures A and B for the submonomer elongation steps and procedure C for the final N-terminal acetylation. Peptoid **7** was isolated as a white solid after purification by flash column chromatography on silica gel. (110 mg, 0.12 mmol); $R_f = 0.85$ (EtOAc). m.p. 134.7-135.2 °C. HRMS (TOF MS ES+) m/z calcd for $C_{51}H_{89}N_6O_8$ $[M+H]^+$: 913.6736; found: 913.6724 Analytical HPLC purity 98%.

1H NMR (400 MHz, $CDCl_3$) δ (ppm): 0.73-1.18 (m, 33H, $CH(CH_3)C(CH_3)_3$ and $CH(CH_3)C(CH_3)_3$ *cis* rotamer), 1.22-1.32 (m, 3H, $CH(CH_3)C(CH_3)_3$ *trans* rotamer), 1.33-1.53 (m, 27H, *Nt*Bu), 1.95-2.16 (m, 3H, $COCH_3$), 3.25-4.56 (m, 13.0H, NCH_2CO and H methyne *trans* rotamer), 4.74 (s, 2H, OCH_2Ph), 5.01-5.31 (m, 2.0H, H methyne *cis* rotamer), 7.28-7.45 (m, 5H, Ph).

Peptoid hexamer 8 (Ac-*Nt*Bu-*Ns*1tbe-*Nt*Bu -*Ns*1tbe-*Nt*Bu-*Ns*1tbe-*OH*). To a solution of peptoid **7** (50 mg, 0.055 mmol) in MeOH (5 mL), carefully purged with argon was added a catalytic amount of 10% Pd/C (5 mg). The suspension was then stirred for 30 min under an atmosphere of hydrogen. The mixture was filtered through a plug of celite which was rinsed with MeOH. The solvent was removed *in vacuo* to yield peptoid **8** as a white solid after purification by flash column chromatography on silica gel. (45.5 mg, 0.054 mmol); $R_f = 0.50$ (EtOAc). m.p. 213.9-214.4 °C. HRMS (TOF MS ES+) m/z calcd for $C_{44}H_{83}N_6O_8$ $[M+H]^+$: 823.6266; found: 823.6267. Analytical HPLC purity 96%.

1H NMR (400 MHz, $CDCl_3$) δ (ppm): 0.78-1.13 (m, 34.1H, $CH(CH_3)C(CH_3)_3$ and $CH(CH_3)C(CH_3)_3$ *cis* rotamer), 1.23-1.51 (m, 28.9H, *Nt*Bu and $CH(CH_3)C(CH_3)_3$ *trans* rotamer),

2.01-2.34 (m, 3H, COCH₃), 3.29-4.51 (m, 12.63H, NCH₂CO and H methyne *trans* rotamer), 4.58-4.80 (m, 2.37H, H methyne *cis* rotamer), 11.64 (bs, 1H, CO₂H).

Peptoid hexamer 9 (Ac-*Nt*Bu-*Nt*Bu-*Ns*1tbe-*Ns*1tbe-*Nt*Bu-*Nt*Bu-*Ot*Bu). The peptoid **9** was synthesized in 12 steps from *tert*-butyl bromoacetate (264 mg, 1.35 mmol) according to procedures A and B for the submonomer elongation steps and procedure C for the final N-terminal acetylation. Peptoid **9** was isolated as a white solid after purification by flash column chromatography on silica gel. (248 mg, 0.29 mmol); *R_f* = 0.84 (EtOAc). m.p. 144.3-144.7°C. HRMS (TOF MS ES+) *m/z* calcd for C₄₆H₈₇N₆O₈ [M+H]⁺: 851.6580; found: 851.6578. Analytical HPLC purity 99%.

¹H NMR (400 MHz, CDCl₃) δ (ppm): 0.84-0.94 (m, 18H, CH(CH₃)C(CH₃)₃), 0.98-1.07 (m, 6H CH(CH₃)C(CH₃)₃ *cis* rotamer), 1.35-1.46 (m, 36H, *Nt*Bu), 1.50 (s, 9H, CO_{2t}Bu), 1.88- 2.04 (m, 3H, COCH₃), 3.37-4.40 (m, 12H, NCH₂CO), 4.57-4.79 (m, 2H, H methyne *cis* rotamer).

Peptoid heptamer 10 (Ac-*Nt*Bu-*Nt*Bu-*Ns*1tbe-*Ns*1tbe-*Ns*1tbe-*Nt*Bu-*Nt*Bu-*Ot*Bu). The peptoid **10** was synthesized in 14 steps from *tert*-butyl bromoacetate (264 mg, 1.35 mmol) according to procedures A and B for the submonomer elongation steps and procedure C for the final N-terminal acetylation. Peptoid **10** was isolated as a white foam after purification by flash column chromatography on silica gel. (178 mg, 0.18 mmol); *R_f* = 0.80 (EtOAc). HRMS (TOF MS ES+) *m/z* calculated for C₅₄H₁₀₁N₇O₉Na [M+Na]⁺: 1014.7553; found: 1014.7476. Analytical HPLC purity 97%.

¹H NMR (400 MHz, CDCl₃) δ (ppm): 0.84-1.08 (m, 36H, CH(CH₃)C(CH₃)₃ and CH(CH₃)C(CH₃)₃ *cis* rotamer), 1.36-1.47 (m, 36H, *Nt*Bu), 1.51 (s, 9H, CO_{2t}Bu), 1.90- 2.10 (m, 3H, COCH₃), 3.70-4.37 (m, 19H, NCH₂CO), 4.61-4.86 (m, 3H, H methyne *cis* rotamer).

Peptoid nonamer 11 (Ac-*Nt*Bu-*Nt*Bu-*Nt*Bu-*Ns*1tbe-*Ns*1tbe-*Ns*1tbe-*Nt*Bu-*Nt*Bu-*Nt*Bu-*Ot*Bu). The peptoid **11** was synthesized in 17 steps from *tert*-butyl bromoacetate (264 mg, 1.35 mmol) according to procedures A and B for the submonomer elongation steps and procedure C for the final N-terminal acetylation. Peptoid **11** was isolated as a white solid after purification by flash column chromatography on silica gel. (252 mg, 0.21 mmol); *R_f* = 0.87 (EtOAc). m.p. 165.9-166.7°C HRMS (TOF MS ES+) *m/z* calcd for C₆₆H₁₂₄N₉O₁₁ [M+H]⁺: 1218.9342; found: 1218.9441. Analytical HPLC purity 95%.

¹H NMR (400 MHz, CDCl₃) δ (ppm): 0.81-1.08 (m, 36H, CH(CH₃)C(CH₃)₃ and CH(CH₃)C(CH₃)₃ *cis* rotamer), 1.32-1.49 (m, 54H, *Nt*Bu), 1.52 (s, 9H, CO_{2t}Bu), 1.89- 2.10 (m, 3H, COCH₃), 3.42-4.39 (m, 14 H, NCH₂CO), 4.62-4.82 (m, 3H, H methyne *cis* rotamer).

Peptoid trimer 12 (Ac-*Nt*Bu-*Ns*1tbe-*Ns*1tbe-*Ot*Bu). The peptoid **12** was synthesized in 6 steps from *tert*-butyl bromoacetate (74 mg, 0.38 mmol) according to procedures A and B for the submonomer elongation steps and procedure C for the final N-terminal acetylation. Peptoid **12** was isolated as a white solid after purification by flash column chromatography on silica gel. (94 mg, 0.18 mmol); R_f =0.48 (EtOAc/cyclohexane 60:40). m.p. 200-201 °C HRMS (TOF MS ES+) m/z calcd for $C_{28}H_{54}N_3O_5$ $[M+H]^+$: 512.4058; found: 512.4059. Analytical HPLC purity 99%.

1H NMR (400 MHz, $CDCl_3$) δ (ppm): 0.84-1.10 (m, 21.9H, $CH(CH_3)C(CH_3)_3$ and $CH(CH_3)C(CH_3)_3$ *cis* rotamer), 1.21-1.28 (m, 2.1H, $CH(CH_3)C(CH_3)_3$ *trans* rotamer), 1.39-1.52 (m, 18H, *Nt*Bu and CO_2t Bu), 1.93-2.06 (m, 3H, $COCH_3$), 3.48-3.61 (m, 0.70H, H methyne *trans* rotamer), 3.70-4.36 (m, 6H, NCH_2CO), 4.64-4.82 (m, 1.30H, H methyne *cis* rotamer).

Peptoid tetramer 13 (Ac-*Ns*1tbe-*Nt*Bu-*Ns*1tbe-*Ns*1tbe-*Ot*Bu). The peptoid **13** was synthesized in 8 steps from *tert*-butyl bromoacetate (70 mg, 0.36 mmol) according to procedures A and B for the submonomer elongation steps and procedure C for the final N-terminal acetylation. Peptoid **13** was isolated as a white solid after purification by flash column chromatography on silica gel. (56 mg, 0.08 mmol); R_f =0.53 (EtOAc/cyclohexane 60:40). m.p. 118.3-118.9 °C HRMS (TOF MS ES+) m/z calcd for $C_{36}H_{69}N_4O_6$ $[M+H]^+$: 653.5211; found: 653.5214. Analytical HPLC purity 99%.

1H NMR (400 MHz, $CDCl_3$) δ (ppm): 0.84-1.10 (m, 33.06H, $CH(CH_3)C(CH_3)_3$ and $CH(CH_3)C(CH_3)_3$ *cis* rotamer), 1.22-1.32 (m, 2.94H, $CH(CH_3)C(CH_3)_3$ *trans* rotamer), 1.35-1.55 (m, 18H, *Nt*Bu and CO_2t Bu), 1.89-2.06 (m, 2.02H, $COCH_3$), 2.11-2.18 (m, 0.98H, $COCH_3$), 3.34-4.41 (m, 8.98H, NCH_2CO and H methyne *trans* rotamer), 4.61-4.81 (m, 2.02H, H methyne *cis* rotamer).

Peptoid pentamer 14 (Ac-*Ns*1tbe-*Ns*1tbe-*Nt*Bu-*Ns*1tbe-*Ns*1tbe-*Ot*Bu). The peptoid **14** was synthesized in 10 steps from *tert*-butyl bromoacetate (96 mg, 0.49 mmol) according to procedures A and B for the submonomer elongation steps and procedure C for the final N-terminal acetylation. Peptoid **14** was isolated as a white solid after purification by flash column chromatography on silica gel. (67mg, 0.08 mmol); R_f = 0.60 (EtOAc). m.p. 224-225 °C. HRMS (TOF MS ES+) m/z calcd for $C_{44}H_{84}N_5O_7$ $[M+H]^+$: 794.6365; found: 794.6371. Analytical HPLC purity 98%.

1H NMR (400 MHz, $CDCl_3$) δ (ppm): 0.78-1.12 (m, 45.36H, $CH(CH_3)C(CH_3)_3$ and $CH(CH_3)C(CH_3)_3$ *cis* rotamer), 1.22-1.60 (m, 20.64H, *Nt*Bu and CO_2t Bu and $CH(CH_3)C(CH_3)_3$ *trans* rotamer), 1.92-2.08 (m, 2.31H, $COCH_3$), 2.12-2.24 (m, 0.69H, $COCH_3$), 3.34-4.46 (m, 10.88H, NCH_2CO and H methyne *trans* rotamer), 4.60-4.86 (m, 3.12H, H methyne *cis* rotamer).

Peptoid hexamer 15 (Ac-*Nt*Bu-*Ns*1tbe-*Ns*1tbe-*Nt*Bu-*Ns*1tbe-*Ns*1tbe-*Ot*Bu). The peptoid **15** was synthesized in 12 steps from *tert*-butyl bromoacetate (97 mg, 0.49 mmol) according to procedures A and B for the submonomer elongation steps and procedure C for the final N-terminal acetylation. Peptoid **15** was isolated as a white solid after purification by flash column chromatography on silica gel. (42 mg, 0.046 mmol); $R_f = 0.66$ (100% EtOAc). m.p. 135.8-136.5 °C. HRMS (TOF MS ES+) m/z calcd for $C_{50}H_{95}N_6O_8$ $[M+H]^+$: 907.7205; found: 907.7216. Analytical HPLC purity 98%.

1H NMR (400 MHz, $CDCl_3$) δ (ppm): 0.79-1.26 (m, 48H, $CH(CH_3)C(CH_3)_3$), 1.27-1.55 (m, 27H, *Nt*Bu and CO_2t Bu), 1.93-2.14 (m, 3H, $COCH_3$), 3.45-4.30 (m, 12.69H, NCH_2CO and H methyne *trans* rotamer), 4.62-4.77 (m, 3.31H, H methyne *cis* rotamer).

Peptoid nonamer 16 (Ac-*Nt*Bu-*Ns*1tbe-*Ns*1tbe-*Nt*Bu-*Ns*1tbe-*Ns*1tbe-*Nt*Bu-*Ns*1tbe-*Ns*1tbe-*Ot*Bu). The peptoid **16** was synthesized in 18 steps from *tert*-butyl bromoacetate (292 mg, 1.50 mmol) according to procedures A and B for the submonomer elongation steps and procedure C for the final N-terminal acetylation. Peptoid **16** was isolated as a white solid after purification by flash column chromatography on silica gel. (22 mg, 0.017 mmol); $R_f = 0.55$ (100% EtOAc). m.p. 153.4-154.0 °C. HRMS (TOF MS ES+) m/z calcd for $C_{72}H_{136}N_9O_{11}$ $[M+H]^+$: 1303.0353; found: 1303.0353. Analytical HPLC purity 99%.

1H NMR (400 MHz, $CDCl_3$) δ (ppm): 0.76-1.16 (m, 72H, $CH(CH_3)C(CH_3)_3$), 1.31-1.51 (m, 36H, *Nt*Bu and CO_2t Bu), 1.91-2.03(m, 3H, $COCH_3$), 3.39-4.37 (m, 19.2H, NCH_2CO and H methyne *trans* rotamer), 4.60- 4.81(m, 4.8H, H methyne *cis* rotamer).

ASSOCIATED CONTENT

General synthetic scheme, HPLC traces, 1H NMR and HSQCAD spectra, CD of a number of different peptoid oligomers, crystal structure report for peptoids **12** and **14**.

X-ray crystallographic data for compounds **12** (CCDC 1960900) (CIF) and **14** (CCDC 1960948) (CIF).

AUTHOR INFORMATION

ORCID

Claude Taillefumier: [0000-0003-3126-495X](https://orcid.org/0000-0003-3126-495X)

ACKNOWLEDGEMENTS

We thank Aurélie Job for HPLC measurements and Martin Leremboire (UCA Partner) for LCMS. M.R. was supported by a grant from the Ministry for Higher Education and Scientific

Research of Tunisia. We acknowledge use of the UMS2008-IBSLor Biophysics and Structural Biology core facility at Université de Lorraine for CD measurements.

-
- ¹ Culf, A. S.; Ouellette, R. J. Solid-Phase Synthesis of N-Substituted Glycine Oligomers (alpha-Peptoids) and Derivatives. *Molecules* **2010**, *15*, 5282-5335.
- ² Knight, A. S.; Zhou, E. Y.; Francis, M. B.; Zuckermann, R. N. Sequence Programmable Peptoid Polymers for Diverse Materials Applications. *Adv. Mater.* **2015**, *27*, 5665-5691.
- ³ Gangloff, N.; Ulbricht, J.; Lorson, T.; Schlaad, H.; Luxenhofer, R. Peptoids and Polypeptoids at the Frontier of Supra- and Macromolecular Engineering. *Chem. Rev.* **2016**, *116*, 1753-1802.
- ⁴ Zuckermann, R. N.; Kodadek, T. Peptoids as potential therapeutics. *Curr. Opin. Mol. Ther.* **2009**, *11*, 299-307.
- ⁵ Dohm, M. T.; Kapoor, R.; Barron, A. E. Peptoids: Bio-Inspired Polymers as Potential Pharmaceuticals. *Curr. Pharm. Des.* **2011**, *17*, 2732-2747.
- ⁶ Horne, W. S. Peptide and peptoid foldamers in medicinal chemistry. *Expert Opin. Drug Dis.* **2011**, *6*, 1247-1262.
- ⁷ Maayan, G.; Ward, M. D.; Kirshenbaum, K. Metallopeptoids. *Chem. Commun.*, **2009**, 56-58.
- ⁸ Maayan, G.; Ward, M. D.; Kirshenbaum, K. Folded biomimetic oligomers for enantioselective catalysis. *Proc. Natl. Acad. Sci. USA* **2009**, *106*, 13679-13684.
- ⁹ Zborovsky, L.; Tigger-Zaborov, H.; Maayan, G. Sequence and Structure of Peptoid Oligomers Can Tune the Photoluminescence of an Embedded Ruthenium Dye. *Chem. Eur. J.* **2019**, *25*, 9098-9107.
- ¹⁰ Zuckermann, R. N.; Kerr, J. M.; Kent, S. B. H.; Moos, W. H. Efficient method for the preparation of peptoids [oligo(N-substituted glycines)] by submonomer solid-phase synthesis. *J. Am. Chem. Soc.* **1992**, *114*, 10646-10647.
- ¹¹ Miller, S. M.; Simon, R. J.; Ng, S.; Zuckermann, R. N.; Kerr, J. M.; Moos, W. H. Proteolytic Studies of Homologous Peptide and N-Substituted Glycine Peptoid Oligomers. *Bioorg. Med. Chem. Lett.* **1994**, *4*, 2657-2662.
- ¹² Miller, S. M.; Simon, R. J.; Ng, S.; Zuckermann, R. N.; Kerr, J. M.; Moos, W. H. Comparison of the Proteolytic Susceptibilities of Homologous L-Amino-Acid, D-Amino-Acid, and N-Substituted Glycine Peptide and Peptoid Oligomers. *Drug Dev. Res.* **1995**, *35*, 20-32.
- ¹³ Armand, P.; Kirshenbaum, K.; Goldsmith, R. A.; Farr-Jones, S.; Barron, A. E.; Truong, K. T. V.; Dill, K. A.; Mierke, D. F.; Cohen, F. E.; Zuckermann, R. N.; Bradley, E. K. NMR determination of the major solution conformation of a peptoid pentamer with chiral side chains. *Proc. Natl. Acad. Sci. USA* **1998**, *95*, 4309-4314.
- ¹⁴ Wu, C. W.; Kirshenbaum, K.; Sanborn, T. J.; Patch, J. A.; Huang, K.; Dill, K. A.; Zuckermann, R. N.; Barron, A. E. Structural and spectroscopic studies of peptoid oligomers with α -chiral aliphatic side chains. *J. Am. Chem. Soc.* **2003**, *125*, 13525-13530.
- ¹⁵ Stringer, J. R.; Crapster, J. A.; Guzei, I. A.; Blackwell, H. E. Extraordinarily Robust Polyproline Type I Peptoid Helices Generated via the Incorporation of alpha-Chiral Aromatic N-1-Naphthylethyl Side Chains. *J. Am. Chem. Soc.* **2011**, *133* (39), 15559-15567.
- ¹⁶ Roy, O.; Dumonteil, G.; Faure, S.; Jouffret, L.; Kriznik, A.; Taillefumier, C. Homogeneous and Robust Polyproline Type I Helices from Peptoids with Nonaromatic α -Chiral Side Chains. *J. Am. Chem. Soc.* **2017**, *139*, 13533-13540.
- ¹⁷ Shah, N. H.; Butterfoss, G. L.; Nguyen, K.; Yoo, B.; Bonneau, R.; Rabenstein, D. L.; Kirshenbaum, K. Oligo(N-aryl glycines): A New Twist on Structured Peptoids. *J. Am. Chem. Soc.* **2008**, *130*, 16622-16632.
- ¹⁸ Crapster, J. A.; Stringer, J. R.; Guzei, I. A.; Blackwell, H. E. Design and Conformational Analysis of Peptoids Containing N-Hydroxy Amides Reveals a Unique Sheet-Like Secondary Structure. *Biopolymers* **2011**, *96*, 604-616.
- ¹⁹ (a) Shin, S. B.; Yoo, B.; Todaro, L. J.; Kirshenbaum, K. Cyclic Peptoids. *J. Am. Chem. Soc.* **2007**, *129*, 3218-3225. (b) D'Amato, A.; Pierri, G.; Tedesco, C.; Della Sala, G.; Izzo, I.; Costabile, C.; De Riccardis, F. Reverse Turn and Loop Secondary Structures in Stereodefined Cyclic Peptoid Scaffolds. *J. Org. Chem.* **2019**, *84*, 10911-10928. (c) Huang, K.; Wu, C. W.; Sanborn, T. J.; Patch, J. A.; Kirshenbaum, K.; Zuckermann, R. N.; Barron, A. E.; Radhakrishnan, I. A Threaded Loop Conformation Adopted by a Family of Peptoid Nonamers. *J. Am. Chem. Soc.* **2006**, *128*, 1733-1738.
- ²⁰ Gorske, B. C.; Mumford, E. M.; Gerrity, C. G.; Ko, I. A Peptoid Square Helix via Synergistic Control of Backbone Dihedral Angles. *J. Am. Chem. Soc.* **2017**, *139*, 8070-8073.
- ²¹ Crapster, J. A.; Guzei, I. A.; Blackwell, H. E. A Peptoid Ribbon Secondary Structure. *Angew. Chem. Int. Ed.* **2013**, *52* (19), 5079-5084.
- ²² Gorske, B. C.; Mumford, E. M.; Conry, R. R. Tandem Incorporation of Enantiomeric Residues Engenders Discrete Peptoid Structures. *Org. Lett.* **2016**, *18*, 2780-2783.
- ²³ Sui, Q.; Borchardt, D.; Rabenstein, D. L. Kinetics and Equilibria of Cis/Trans Isomerization of Backbone Amide Bonds in Peptoids. *J. Am. Chem. Soc.* **2007**, *129*, 12042-12048.

-
- ²⁴ Butterfoss, G. L.; Renfrew, P. D.; Kuhlman, B.; Kirshenbaum, K.; Bonneau, R. A Preliminary Survey of the Peptoid Folding Landscape. *J. Am. Chem. Soc.* **2009**, *131*, 16798-16807.
- ²⁵ Gorske, B. C.; Bastian, B. L.; Geske, G. D.; Blackwell, H. E. Local and tunable n \rightarrow pi* interactions regulate amide isomerism in the peptoid backbone. *J. Am. Chem. Soc.* **2007**, *129*, 8928-8929.
- ²⁶ Gorske, B. C.; Stringer, J. R.; Bastian, B. L.; Fowler, S. A.; Blackwell, H. E. New Strategies for the Design of Folded Peptoids Revealed by a Survey of Noncovalent Interactions in Model Systems. *J. Am. Chem. Soc.* **2009**, *131*, 16555-16567.
- ²⁷ Stringer, J. R.; Crapster, J. A.; Guzei, I. A.; Blackwell, H. E. Construction of Peptoids with All Trans-Amide Backbones and Peptoid Reverse Turns via the Tactical Incorporation of N-Aryl Side Chains Capable of Hydrogen Bonding. *J. Org. Chem.* **2010**, *75*, 6068-6078.
- ²⁸ Caumes, C.; Roy, O.; Faure, S.; Taillefumier, C. The Click Triazolium Peptoid Side Chain: A Strong cis-Amide Inducer Enabling Chemical Diversity. *J. Am. Chem. Soc.* **2012**, *134*, 9553-9556.
- ²⁹ Roy, O.; Caumes, C.; Esvan, Y.; Didierjean, C.; Faure, S.; Taillefumier, C. The tert-Butyl Side Chain: A Powerful Means to Lock Peptoid Amide Bonds in the Cis Conformation. *Org. Lett.* **2013**, *15*, 2246-2249.
- ³⁰ Angelici, G.; Bhattacharjee, N.; Roy, O.; Faure, S.; Didierjean, C.; Jouffret, L.; Jolibois, F.; Perrin, L.; Taillefumier, C. Weak backbone CH \cdots O=C and side chain tBu \cdots tBu London interactions help promote helix folding of achiral NtBu peptoids. *Chem. Commun.* **2016**, *52*, 4573-4576.
- ³¹ Gimenez, D.; Aguilar, J. A.; Bromley, E. H.; Cobb, S. L. Stabilising Peptoid Helices Using Non-Chiral Fluoroalkyl Monomers. *Angew. Chem. Int. Ed.* **2018**, *57*, 10549-10553.
- ³² Kuemin, M.; Engel, J.; Wennemers, H. Temperature-induced transition between polyproline I and II helices: quantitative fitting of hysteresis effects. *J. Peptide Sci.* **2010**, *16*, 596-600.
- ³³ Armand, P.; Kirshenbaum, K.; Falicov, A.; Dunbrack Jr, R. L.; Dill, K. A.; Zuckermann, R. N.; Cohen, F. E. Chiral N-substituted glycines can form stable helical conformations. *Fold. Des.* **1997**, *2*, 369-375.
- ³⁴ Baskin, M.; Maayan, G. A rationally designed metal-binding helical peptoid for selective recognition processes. *Chem. Sci.* **2016**, *7*, 2809-2820.
- ³⁵ Tigger-Zaborov, H.; Maayan, G. Aggregation of Ag(0) nanoparticles to unexpected stable chain-like assemblies mediated by 2,2'-bipyridine decorated peptoids. *J. Colloid Interf. Sci.* **2019**, *533*, 598-603.
- ³⁶ Wu, C. W.; Sanborn, T. J.; Huang, K.; Zuckermann, R. N.; Barron, A. E. Peptoid oligomers with α -chiral, aromatic side chains: Sequence requirements for the formation of stable peptoid helices. *J. Am. Chem. Soc.* **2001**, *123*, 6778-6784.
- ³⁷ Wu, C. W.; Sanborn, T. J.; Zuckermann, R. N.; Barron, A. E. Peptoid Oligomers with α -Chiral, Aromatic Side Chains: Effects of Chain Length on Secondary Structure. *J. Am. Chem. Soc.* **2001**, *123*, 2958-2963.
- ³⁸ Shin, H. M.; Kang, C. M.; Yoon, M. H.; Seo, J. Peptoid helicity modulation: precise control of peptoid secondary structures via position-specific placement of chiral monomers. *Chem. Commun.* **2014**, *50* (34), 4465-4468.
- ³⁹ Green, M. M.; Reidy, M. P.; Johnson, R. D.; Darling, G.; O'Leary, D. J.; Willson, G. Macromolecular stereochemistry: the out-of-proportion influence of optically active comonomers on the conformational characteristics of polyisocyanates. The sergeants and soldiers experiment. *J. Am. Chem. Soc.* **1989**, *111*, 6452-6454.
- ⁴⁰ Shyam, R.; Nauton, L.; Angelici, G.; Roy, O.; Taillefumier, C.; Faure, S. NC α -gem-dimethylated peptoid side chains: A novel approach for structural control and peptide sequence mimetics. *Biopolymers* **2019**, *110*, e23273.
- ⁴¹ Hjelmggaard, T.; Faure, S.; Caumes, C.; De Santis, E.; Edwards, A. A.; Taillefumier, C. Convenient Solution-Phase Synthesis and Conformational Studies of Novel Linear and Cyclic α,β -Alternating Peptoids. *Org. Lett.* **2009**, *11*, 4100-4103.
- ⁴² Gorske, B. C.; Blackwell, H. E. Tuning peptoid secondary structure with pentafluoroaromatic functionality: A new design paradigm for the construction of discretely folded peptoid structures *J. Am. Chem. Soc.* **2006**, *128*, 14378-14387.

TOC graphic

